

# Towards Symbiotic SAGIN Through Inter-operator Resource and Service Sharing: Joint Orchestration of User Association and Radio Resources

Shizhao He, Jungang Ge, Ying-Chang Liang, *Fellow, IEEE*, and Dusit Niyato, *Fellow, IEEE*

**Abstract**—The space-air-ground integrated network (SAGIN) is a pivotal architecture to support ubiquitous connectivity in the upcoming 6G era. Inter-operator resource and service sharing is a promising way to realize such a huge network, utilizing resources efficiently and reducing construction costs. Given the rationality of operators, the configuration of resources and services in SAGIN should focus on both the overall system performance and individual benefits of operators. Motivated by emerging symbiotic communication facilitating mutual benefits across different radio systems, we investigate the resource and service sharing in SAGIN from a symbiotic communication perspective in this paper. In particular, we consider a SAGIN consisting of a ground network operator (GNO) and a satellite network operator (SNO). Specifically, we aim to maximize the weighted sum rate (WSR) of the whole SAGIN by jointly optimizing the user association, resource allocation, and beamforming. Besides, we introduce a sharing coefficient to characterize the revenue of operators. Operators may suffer revenue loss when only focusing on maximizing the WSR. In pursuit of mutual benefits, we propose a mutual benefit constraint (MBC) to ensure that each operator obtains revenue gains. Then, we develop a centralized algorithm based on the successive convex approximation (SCA) method. Considering that the centralized algorithm is difficult to implement, we propose a distributed algorithm based on Lagrangian dual decomposition and the consensus alternating direction method of multipliers (ADMM). Finally, we provide extensive numerical simulations to demonstrate the effectiveness of the two proposed algorithms, and the distributed optimization algorithm can approach the performance of the centralized one. The results also reveal that the proposed MBCs can enable operators to achieve mutual benefits and realize a symbiotic resource and service sharing paradigm.

**Index Terms**—Symbiotic communication, SAGIN, inter-operator resource and service sharing, resource optimization.

## I. INTRODUCTION

Wireless communication has made outstanding achievements in the past decades and stepped into the 5G era. Although 5G can realize much better performance than former communication systems, including higher peak data rate, and ultra reliable and low latency, it still cannot satisfy some requirements in 6G, such as the ubiquitous connectivity [1]. In fact, there are still 2.7 billion people who cannot access the Internet, and about 6% of the rural area worldwide lacks

mobile network coverage [2]. The principal reasons are the limited coverage of ground networks and the high expenses of deploying networks in rural areas. Satellite networks have emerged as an important complementary technology to enhance coverage of ground networks [3], which can tackle the above issues. Compared with ground networks, satellite networks can provide seamless coverage to users without deploying costly fiber optic backhaul. Therefore, the space-air-ground integrated network (SAGIN) is a vital technology to realize ubiquitous connectivity in the 6G era.

Recently, satellite networks have rapidly developed and attracted considerable attention from academia to industry. For instance, SpaceX has launched over 4,000 low earth orbit (LEO) satellites to construct Starlink [4]. To realize ubiquitous connectivity, addressing the severe path loss caused by the long propagation distance is necessary. In Starlink, a satellite terminal (ST) comprising a satellite dish and an access point is exploited to deal with this problem. The satellite dish provides high antenna gain to compensate for the path loss, and the access point offers access service to users. In [5], a satellite access network for 5G and beyond is proposed based on this kind of ST. Satellite networks are also expected to realize high throughput satellite communication. To this end, high frequency is adopted in satellite communication, such as Ka band [6]. Besides, multi-beam satellites also play an essential role in realizing high throughput satellite communication. Compared with conventional satellites, multi-beam satellites can generate multiple beams with high gain and thus provide better satellite communication [7], [8]. Moreover, the shadowed-Rician (SR) fading is widely adopted to model the satellite-ground channels, based on which many works analyze the performance of satellite networks [9]–[11]. Resource allocation in satellite networks is also widely studied [12], [13]. Additionally, diverse multiple access techniques are adopted in satellite networks to serve users [14], [15], such as the time division multiple access (TDMA) manner.

The rapid growth of satellite networks paves the way for realizing SAGIN, which has been widely studied in recent years. Since SAGIN is a large-scale network, it is almost impossible for an individual network operator to construct it. Therefore, inter-operator sharing<sup>1</sup> is a promising technology for constructing SAGIN. In fact, the famous ground network operator (GNO) T-mobile announces that it aims to provide seamless coverage to users by cooperating with satellite network operator (SNO) SpaceX [16]. Optimizing the

<sup>1</sup>For ease of notation, “inter-operator sharing” is synonymous with “inter-operator resource and service sharing” in this paper.

This work has been submitted to the IEEE for possible publication. Copyright may be transferred without notice, after which this version may no longer be accessible.

S. He, J. Ge, and Y.-C. Liang are with the National Key Laboratory of Wireless Communications, and the Center for Intelligent Networking and Communications (CINC), University of Electronic Science and Technology of China (UESTC), Chengdu 611731, China (e-mail: heshizhao@std.uestc.edu.cn; gejungang@std.uestc.edu.cn; liangyc@ieee.org).

Dusit Niyato is with the School of Computer Science and Engineering, Nanyang Technological University (NTU), Singapore (e-mail: dniyato@ntu.edu.sg)

configuration of resources and services is an essential problem to fully exploit the advantages of SAGIN with inter-operator sharing. Considering the limited spectrum, many works study the spectrum sharing problem in SAGIN [17]–[19]. In [18], catering to the heterogeneity and high dynamics of SAGIN, the authors propose an intelligent spectrum management framework empowered by artificial intelligence and software defined network (SDN). In [20], the spectrum allocation is optimized to maximize the sum rate while reducing the interference received at satellite users. On the other hand, service sharing is another critical topic in studying SAGIN. Many recent scientific literatures demonstrate that satellite networks are a promising supplement to ground networks in providing diversity services to remote areas, such as backhaul connectivity [21]–[23] and task offloading [24], [25]. In [23], a satellite assists ground networks in providing backhaul links to users in remote areas, and both user association and beamforming are optimized to maximize the sum rate. In [25], satellite networks support task offloading of remote Internet-of-Things (IoT) devices. An optimization problem about user association and spectrum allocation is formulated to minimize the task offloading delay. The above works only focus on the overall performance of SAGIN. However, motivating different operators to share resources and services is also a vital problem. As the operators are inherently competitors with conflicting interests, they will be reluctant to construct SAGIN if resource and service sharing cannot guarantee their revenue, i.e., they cannot achieve mutual benefits. In [26], a pricing mechanism is proposed to ensure each operator’s revenue. However, it cannot fully leverage the resources in SAGIN to achieve a high overall performance. Therefore, it is vital to simultaneously achieve mutual benefits among operators and maximize the overall performance of SAGIN.

The recently emerging symbiotic communication provides a promising paradigm to tackle the above problem, which aims to optimize the collective objectives of diverse radio systems and realize mutual benefits among them via sharing resources and services [27]. Symbiotic communication has been widely studied in backscatter communications [28]–[32]. In [28], the authors investigate the symbiotic communication in a passive IoT system, consisting of an active transmission and a backscatter transmission. Specifically, the active transmission shares spectrum and energy resources with the backscatter transmission, and in return the backscatter transmission provides a beneficial multi-path to the active transmission via reflecting the incident signal. As a result, the active and backscatter transmission achieve mutual benefits in this system, realizing higher sum rate. Besides, the symbiotic communication is realized in the coexistence of a cellular network and WiFi system in [33]. Particularly, the WiFi system shares spectrum with the cellular network, and the cellular network adjusts transmission parameters to guarantee the performance of WiFi system. Resource allocation in symbiotic communication is also studied. In [34], [35], both user association and beamforming are optimized to realize the symbiotic communication in multi-operator cellular networks. Symbiotic communication can also be a prominent solution to construct SAGIN. In [36], the authors propose a

blockchain and deep learning based framework to optimize resource allocation in SAGIN with the guidance of symbiotic communication. However, it lacks an explicit formulation to strictly guarantee individual benefits after sharing resources and services.

Motivated by the above works, in this paper, we investigate joint user association, resource allocation, and beamforming design in SAGIN from a symbiotic communication perspective. Specifically, the considered SAGIN system consists of a GNO and SNO engaging in inter-operator sharing, i.e., sharing spectrum and allowing users to access arbitrary networks. The GNO has base stations (BSs) connected to the core network by fiber. On the other hand, the SNO has STs connected to the core network via a multi-beam LEO satellite, and this LEO satellite serves STs in the TDMA manner. Given the high cost of deploying fiber in remote areas, the number of BSs is fewer than that of STs. Our objective is to maximize the weighted sum rate (WSR) of all users while achieving mutual benefits among operators in terms of revenue. To characterize revenue of operators, we introduce a sharing coefficient that reflects the impact of inter-operator sharing. The revenue may experience losses when only pursuing the maximization of the WSR. To achieve mutual benefits, we propose a mutual benefit constraint (MBC) to guarantee that each operator can obtain higher revenue with inter-operator sharing. The main contributions of this work can be summarized as follows:

- We investigate a symbiotic resource and service sharing paradigm in the SAGIN, which aims to maximize the overall system performance and realize mutual benefits between the GNO and SNO. We formulate an optimization problem regarding user association, resource allocation, and beamforming design to maximize the WSR, subject to the MBCs and STs’ backhaul capacity constraints.
- We introduce a sharing coefficient to characterize the revenue of each network operator, based on which the MBC is formulated to ensure each operator can obtain revenue gains after sharing spectrum and services.
- We propose a centralized algorithm based on successive convex approximation (SCA) for the formulated WSR maximization problem. Concerning the large scale of the SAGIN, it is challenging to implement the centralized algorithm. Then, we develop a distributed algorithm, which consists of the Lagrangian dual decomposition based algorithm for user association and consensus alternating direction method of multipliers (ADMM) based algorithm for beamforming design and resource allocation.
- Simulation results show that both the proposed algorithms can outperform the considered benchmarks, and the distributed algorithm approaches a performance close to that of the centralized algorithm. Moreover, in comparison to operators in the non-symbiotic case, each operator in the symbiotic case attains higher revenue after sharing spectrum and services. This implies that operators achieve mutual benefits and realize a symbiotic resource and service sharing paradigm in the SAGIN.

The remainder of this paper is organized as follows. Section

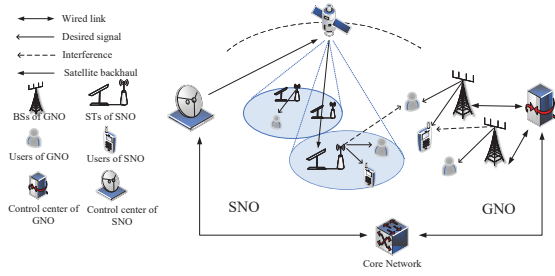


Fig. 1. The considered SAGIN with inter-operator sharing.

II illustrates the system model. In Section III, we formulate the WSR maximization problem for the considered SAGIN system. In Section IV, an SCA-based centralized algorithm and finding initial point algorithm are proposed for the WSR maximization problem. In Section V, a distributed algorithm based on consensus ADMM and Lagrangian dual decomposition methods is developed. In Section VI, the extensive simulation results are presented. Finally, Section VII concludes this paper.

Notations: The notations in this paper are listed as follows. The scalars, column vectors and matrices are represented by lowercase, bold lowercase and uppercase symbols (e.g.,  $x$ ,  $\mathbf{x}$  and  $\mathbf{X}$ ), respectively.  $|\mathcal{A}|$  denotes the cardinality of set  $\mathcal{A}$ .  $\mathbb{C}$  denotes the set of complex numbers. Main notations are summarized in Table I.

## II. SYSTEM MODEL

### A. SAGIN Network

As shown in Fig. 1, we consider the downlink of a SAGIN system, which consists of a GNO and SNO, and we define  $\mathcal{O} = \{G, S\}$  as the set of operators. Specifically, the GNO has  $N_U$  users and deploys  $N_B$  BSs, directly connected to the core network via fiber that can provide large backhaul capacity. On the other hand, the SNO has  $N'_U$  subscribed users and deploys  $N'_B$  STs to serve users in remote areas, and it exploits a multi-beam LEO satellite to provide backhaul links to STs over the Ka band. Since the payload of the satellite is constrained, the backhaul capacity it provides to STs is limited. Besides, both operators have a dedicated C band for serving users. We denote  $\mathcal{B}_G = \{1, 2, \dots, N_B\}$  and  $\mathcal{B}_S = \{N_B + 1, N_B + 2, \dots, N_B + N'_B\}$  as the set of all BSs and STs, respectively. Denote the set of subscribed users of the GNO as  $\mathcal{U}_G = \{1, 2, \dots, N_U\}$  and that of the SNO as  $\mathcal{U}_S = \{N_U + 1, N_U + 2, \dots, N_U + N'_U\}$ . Then, we denote  $\mathcal{B} \triangleq \cup_{n \in \mathcal{O}} \mathcal{B}_n$  and  $\mathcal{U} \triangleq \cup_{n \in \mathcal{O}} \mathcal{U}_n$ . We consider that all BSs and STs are equipped with  $N_t$  transmit antennas while all users are equipped with a single antenna. In the considered SAGIN, inter-operator sharing is adopted, where all BSs and STs share their C bands to serve users, and the users can access arbitrary BSs or STs for service. Furthermore, we assume that each operator has a control center to collect necessary information (e.g., channel state information (CSI), and user locations.).

### B. Space-Ground Communication Model

We consider that the multi-beam LEO satellite is equipped with  $N_L$  feeds, and each can generate a spot beam to provide

backhaul links to STs. Specifically, each beam serves STs within its coverage in the TDMA manner. Besides, universal frequency reuse is adopted in space-ground communication, which means all beams operate over the Ka band. Then, we assume each ST is pointed towards the satellite, and the received signal of ST  $i$  within the coverage of beam  $\ell$  is

$$y_{\ell,i} = \sqrt{p_\ell G_T(\zeta_{\ell,i}) G_R} f_i s_\ell + \sum_{\substack{\ell'=1, \\ \ell' \neq \ell}}^{N_L} \sqrt{p_{\ell'} G_T(\zeta_{\ell',i}) G_R} f_i s_{\ell'} + z_i, \quad (1)$$

where  $p_\ell$  is the transmit power of  $\ell$ -th spot beam;  $s_\ell$  is the symbol transmitted by  $\ell$ -th spot beam, which is assumed to be an independent random variable with zero mean and unit variance; and  $z_i \sim \mathcal{CN}(0, \sigma_s^2)$  is the additive white Gaussian noise (AWGN).  $G_R$  is the receive antenna gain of STs,  $G_T(\zeta_{\ell,i})$  is the transmit antenna gain of the  $\ell$ -th spot beam toward ST  $i$ , and  $\zeta_{\ell,i}$  is the off-boresight angle between the center of  $\ell$ -th spot beam and ST  $i$ . Specifically,  $G_T(\zeta_{\ell,i})$  is given by

$$G_T(\zeta_{\ell,i}) = G_T^0 \cdot 4 \left| \frac{J_1(\kappa a \sin \zeta_{\ell,i})}{\kappa a \sin \zeta_{\ell,i}} \right|^2,$$

where  $G_T^0$  is the maximum transmit gain,  $\kappa = \frac{2\pi}{\lambda_{Ka}}$  is the wave number,  $a$  is the radius of the dish antenna, and  $\lambda_{Ka}$  is the carrier length of Ka band.  $f_i$  is the downlink channel between the LEO satellite and ST  $i$ , which is given by

$$f_i = \sqrt{d_i} \tilde{f}_i, \quad (2)$$

where  $d_i$  accounts for the path-loss between the satellite and ST  $i$ , while  $\tilde{f}_i$  is the SR fading. The probability distribution function of SR fading gain  $|\tilde{f}_i|^2$  is given by

$$f_{|\tilde{f}_i|^2}(s; b, m, \Omega) = \frac{1}{2b} \left( \frac{2bm}{2bm + \Omega} \right)^m \exp\left(-\frac{s}{2b}\right) \times {}_1F_1\left(m, 1, \frac{\Omega s}{2b(2bm + \Omega)}\right), \quad (3)$$

where  $\Omega$  is the average power of a LoS component,  $2b$  is the average power of the scatter components,  $m$  is the Nakagami parameter, and  ${}_1F_1(\cdot, \cdot, \cdot)$  is the confluent hypergeometric function. Based on (1), the backhaul capacity for ST  $i$  served by  $\ell$ -th spot beam is

$$C_{\ell,i} = B_{Ka} t_{\ell,i} \times \log_2 \left( 1 + \frac{p_\ell G_T(\zeta_{\ell,i}) G_R |f_i|^2}{\sum_{\ell' \neq \ell} p_{\ell'} G_T(\zeta_{\ell',i}) G_R |f_i|^2 + \sigma_s^2} \right), \quad (4)$$

where  $B_{Ka}$  denotes the bandwidth of Ka band,  $t_{\ell,i}$  is the fraction of time resource  $\ell$ -th spot beam allocates to ST  $i$ .

### C. Ground-Ground Communication Model

Universal frequency reuse is also adopted by BSs/STs to serve users, and the downlink channel between BS/ST  $i$  and user  $k$  over the spectrum band of operator  $n \in \mathcal{O}$  is given by

$$\mathbf{h}_{i,k}^n = \sqrt{d_{i,k}} \tilde{\mathbf{h}}_{i,k}^n, \quad (5)$$

TABLE I  
MAIN NOTATIONS

Notation	Meaning
$G, S, \mathcal{O}$	GNO, SNO, set of network operators
$\mathcal{B}, \mathcal{B}_G, \mathcal{B}_S$	Set of BSs and STs, set of BSs, set of STs
$\mathcal{U}, \mathcal{U}_G, \mathcal{U}_S$	Set of all users, set of users from GNO, set of users from SNO
$N_B, N'_B$	The number of BSs, the number of STs
$N_U, N'_U$	The number of users from GNO, the number of users from SNO
$N_L, N_t$	The number of feeds of the LEO satellite, the number of transmit antennas of BSs/STs
$P_i, P_{Sat}$	Maximum transmit power of BS/ST $i$ , maximum transmit power of the LEO satellite
$G_T(\cdot), G_R$	Transmit antenna gain of the $\ell$ -th spot beam, receive antenna gain of STs
$f_i$	Downlink channel between the LEO satellite and ST $i$
$\mathbf{h}_{i,k}^n$	Downlink channel between BS/ST $i$ and user $k$ over band $n$
$p_\ell, t_{\ell,i}$	Power of $\ell$ -th spot beam, time allocated to ST $i$ by $\ell$ -th spot beam
$x_{i,k}$	User association variable for BS/ST $i$ and user $k$
$\mathbf{w}_{i,k}^n$	Transmit beamforming that BS/ST $i$ assigns to user $k$ over band $n$
$\delta_z$	Sharing coefficient of operator $z$
$U_z^0, U_z$	Revenue without inter-operator sharing, revenue with inter-operator sharing

where  $d_{i,k}$  is the path-loss between BS/ST  $i$  and user  $k$ , and  $\tilde{\mathbf{h}}_{i,k}^n \in \mathbb{C}^{1 \times N_t}$  is the small-scale fading coefficient. With inter-operator sharing, the users of one operator can access other operators' networks, and each BS/ST can operate over all spectrum bands. In this case, the received signal of user  $k$  associated with BS/ST  $i \in \mathcal{B}_m$  over the band  $n$  is

$$\begin{aligned}
y_{i,k}^n &= \mathbf{h}_{i,k}^n \mathbf{w}_{i,k}^n s_k \\
&+ \sum_{\substack{j \in \mathcal{B}_m, k' \in \mathcal{U} \\ (j,k') \neq (i,k)}} \mathbf{h}_{j,k}^n \mathbf{w}_{j,k'}^n s_{k'} \\
&+ \sum_{j \in \mathcal{B} \setminus \mathcal{B}_m, k' \in \mathcal{U}} \mathbf{h}_{j,k}^n \mathbf{w}_{j,k'}^n s_{k'} + z^n,
\end{aligned} \tag{6}$$

where  $\mathbf{w}_{i,k}^n \in \mathbb{C}^{N_t \times 1}$  is the transmit beamforming that BS/ST  $i$  assigns to user  $k$  over the band  $n$ ;  $s_k$  denotes the symbol transmitted to user  $k$ ; and  $z^n \sim \mathcal{CN}(0, \sigma_t^2)$  is the AWGN over band  $n$ . The instantaneous signal-to-interference-plus-noise ratio (SINR) of user  $k$  in the band  $n$  can be written as

$$\gamma_{i,k}^n = \frac{|\mathbf{h}_{i,k}^n \mathbf{w}_{i,k}^n|^2}{\tilde{I}_{i,k}^n + I_{i,k}^n + \sigma_t^2}, \tag{7}$$

where  $\tilde{I}_{i,k}^n$  denotes the intra-operator interference while  $I_{i,k}^n$  denotes the inter-operator interference. Specifically,  $\tilde{I}_{i,k}^n$  and  $I_{i,k}^n$  are as follows:

$$\tilde{I}_{i,k}^n = \sum_{\substack{j \in \mathcal{B}_m, k' \in \mathcal{U} \\ (j,k') \neq (i,k)}} |\mathbf{h}_{j,k}^n \mathbf{w}_{j,k'}^n|^2, \tag{8a}$$

$$I_{i,k}^n = \sum_{j \in \mathcal{B} \setminus \mathcal{B}_m, k' \in \mathcal{U}} |\mathbf{h}_{j,k}^n \mathbf{w}_{j,k'}^n|^2. \tag{8b}$$

Thus, the achievable rate for user  $k$  with inter-operator sharing is shown as

$$R_{i,k} = \sum_{n \in \mathcal{O}} \log_2(1 + \gamma_{i,k}^n). \tag{9}$$

### III. PROBLEM FORMULATION

As the network performance heavily depends on the configuration of resources and services, we formulate a WSR

maximization (WSRM) problem through jointly optimizing user association, resource allocation, and beamforming design. Specifically, since the backhaul capacity offered by the LEO satellite is limited, the investigated WSRM problem is subject to the backhaul capacity constraints of STs. Besides, we introduce a sharing coefficient  $\delta_z$  for operator  $z$  to characterize its revenue. Based on the revenue, MBCs are proposed to realize mutual benefits, realizing a symbiotic resource and service sharing paradigm.

#### A. Revenue of Operators

While inter-operator sharing can improve the overall performance, it concurrently incurs additional costs due to inter-operator interference and serving other operators' users. Hence, to compensate for the additional costs and incentivize operators to engage in inter-operator sharing, a sharing coefficient  $\delta_z \in [0, 1]$  is introduced for each operator  $z$  to characterize its revenue. As the revenue of an operator is usually related to the transmission rate that it can offer, we define the revenue of operator  $z$  as

$$U_z = \sum_{i \in \mathcal{B}, k \in \mathcal{U}} x_{i,k} \alpha_{i,k}^z R_{i,k}, \tag{10}$$

where  $x_{i,k} \in \{0, 1\}$  is the user association variable,  $x_{i,k} = 1$  if user  $k$  is associated with BS/ST  $i$ , and  $x_{i,k} = 0$  otherwise. Let BS/ST  $i$  belong to operator  $m$ , and user  $k$  subscribe to operator  $n$ , then  $\alpha_{i,k}^z$  is defined as

$$\alpha_{i,k}^z = \begin{cases} 1, & \text{if } z = m = n, \\ \delta_m, & \text{if } z = m, m \neq n, \\ 1 - \delta_m, & \text{if } z = n, m \neq n, \\ 0, & \text{otherwise.} \end{cases} \tag{11}$$

From (10) and (11), it can be observed that the sharing coefficient  $\delta_m$  can affect the revenue (or compensation) obtained by operator  $m$  from serving other operators' users. Thus, this sharing coefficient has a significant impact on service sharing. For example, when  $\delta_m = 0$ , other operators need not compensate operator  $m$  for offloading their users to it, and operator  $m$  cannot obtain any revenue. As a result, for

higher revenue, operator  $m$  prefers to serve its users, while other operators prefer to offload their users to operator  $m$ .

### B. WSRM Formulation

In the studied SAGIN system, each user can be associated with any BSs/STs, and each BS/ST can operate in all bands. To efficiently maximize performance of the whole system while ensuring that operators achieve mutual benefits, we formulate the WSRM problem from the symbiotic communication perspective, which is written as

$$\mathbf{P1} : \max_{\mathbf{p}, \mathbf{t}, \mathbf{W}, \mathbf{x}} \sum_{i \in \mathcal{B}} \sum_{k \in \mathcal{U}} x_{i,k} b_{i,k} R_{i,k} \quad (12a)$$

$$\text{s.t. } U_z \geq U_z^0, \forall z \in \mathcal{O}, \quad (12b)$$

$$\sum_{i \in \mathcal{B}_S} t_{\ell,i} \leq 1, \forall \ell = 1, \dots, N_L, \quad (12c)$$

$$\sum_{k \in \mathcal{U}} B_C R_{i,k} \leq C_{\ell,i}, \forall i \in \mathcal{B}_S, \quad (12d)$$

$$\sum_{n \in \mathcal{O}} \sum_{k \in \mathcal{U}} \|\mathbf{w}_{i,k}^n\|^2 \leq P_i, \forall i \in \mathcal{B}, \quad (12e)$$

$$\sum_{\ell=1}^{N_L} p_{\ell} \leq P_{Sat}, \quad (12f)$$

$$\sum_{i \in \mathcal{B}} x_{i,k} \leq 1, \forall k \in \mathcal{U}, \quad (12g)$$

$$x_{i,k} \in \{0, 1\}, \forall i \in \mathcal{B}, \forall k \in \mathcal{U}, \quad (12h)$$

where  $\mathbf{p} \triangleq \{p_{\ell}\}_{\ell=1,2,\dots,N_L}$ ,  $\mathbf{t} \triangleq \{t_{\ell,i}\}_{\ell=1,2,\dots,N_L, i \in \mathcal{B}_S}$ ,  $\mathbf{w} \triangleq \{\mathbf{w}_{i,k}^n\}_{n \in \mathcal{O}, i \in \mathcal{B}, k \in \mathcal{U}}$ ,  $\mathbf{x} \triangleq \{x_{i,k}\}_{i \in \mathcal{B}, k \in \mathcal{U}}$ ,  $b_{i,k}$  denotes the weight for the rate of user  $k$  associated with BS  $i$ , and  $P_i$  and  $P_{Sat}$  are the maximum transmit power of BS/ST  $i$  and the LEO satellite, respectively. Besides, (12c) is the time resource allocation constraint; (12d) is the backhaul constraint for each ST, and  $B_C$  is the bandwidth of C band; (12e) is the power constraint for each BS/ST, which indicates the spectrum sharing is enabled; (12f) is the power constraint for the LEO satellite; (12g) means that each user can be associated with only one BS/ST, which indicates the service sharing is enabled, and (12h) indicates that  $x_{i,k}$  is a binary variable. Further, (12b) is referred to as the MBC, which ensures that each operator can obtain benefits. Specifically,  $U_z$  is the revenue operator  $z$  can obtain with inter-operator sharing, while  $U_z^0$  is the revenue obtained without inter-operator sharing. The details of determining  $U_z^0$  will be illustrated in Section IV-C.

In the above formulation, we do not take  $x_{i,k}$  into consideration in the left-hand-side (LHS) of constraint (12d) because  $R_{i,k}$  will automatically be 0 when  $x_{i,k} = 0$  at the optimality. To see this, consider the optimal beamforming and user association scheme of  $\mathbf{P1}$  for user  $k$  is  $x_{i,k} = 0$  while  $\mathbf{w}_{i,k}^n \neq 0$ . Since  $x_{i,k}$  is considered in the objective (12a), by setting  $\mathbf{w}_{i,k}^n = 0$ , a feasible solution with higher objective value can be obtained. Then, according to (7) and (9),  $R_{i,k}$  will be 0, too.

## IV. CENTRALIZED OPTIMIZATION ALGORITHMS FOR WSRM

In this section, we leverage the block successive maximization (BSM) method [37] to solve  $\mathbf{P1}$ , where the above

problems are solved in three stages iteratively. In the first stage, the beamforming  $\mathbf{w}$  of BSs/STs and power  $\mathbf{p}$  of the multi-beam LEO satellite are optimized for the given user association scheme  $\mathbf{x}$  and time allocation  $\mathbf{t}$  using the SCA method. Then,  $\mathbf{w}$  and  $\mathbf{t}$  are optimized with fixed  $\mathbf{x}$  and  $\mathbf{p}$ . In the last stage,  $\mathbf{x}$  is optimized for the given beamforming design and resource allocation. Next, we also provide a method to obtain the revenue for each operator without inter-operator sharing ( $U_z^0$ ). Besides, we propose an initial point searching method for the SCA-based algorithm. Finally, the proposed centralized algorithm can be implemented in the assigned control center.

### A. Resource Allocation and Beamforming Optimization for WSRM

$\mathbf{P1}$  is a non-convex and mixed-integer problem, which is hard to tackle. To make the problem tractable, we introduce some auxiliary variables and rewrite  $\mathbf{P1}$  equivalently as

$$\mathbf{P1.1} : \max_{\mathbf{p}, \mathbf{t}, \mathbf{w}, \mathbf{x}, \Gamma, \beta, \varphi, \rho} \sum_{i \in \mathcal{B}} \sum_{k \in \mathcal{U}} x_{i,k} b_{i,k} r_{i,k} \quad (13a)$$

$$\text{s.t. } (12c), (12f), (12g), (12h), \quad (13b)$$

$$\Gamma_{i,k}^n \leq \frac{|\mathbf{h}_{i,k}^n \mathbf{w}_{i,k}^n|^2}{\beta_{i,k}^n}, \quad (13c)$$

$$\beta_{i,k}^n \geq \tilde{I}_{i,k}^n + I_{i,k}^n + \sigma_t^2, \quad (13d)$$

$$\varphi_{i,k}^n \geq \frac{|\mathbf{h}_{i,k}^n \mathbf{w}_{i,k}^n|^2}{\rho_{i,k}^n}, \quad (13e)$$

$$\rho_{i,k}^n \leq \tilde{I}_{i,k}^n + I_{i,k}^n + \sigma_t^2, \quad (13f)$$

$$\sum_{i \in \mathcal{B}} \sum_{k \in \mathcal{U}} x_{i,k} \alpha_{i,k}^z r_{i,k} \geq U_z^0, \quad (13g)$$

$$\sum_{n \in \mathcal{O}} \sum_{k \in \mathcal{U}} B_C \log_2(1 + \varphi_{i,k}^n) \leq C_{\ell,i}, \quad (13h)$$

$$r_{i,k} = \sum_{n \in \mathcal{O}} \log_2(1 + \Gamma_{i,k}^n), \quad (13i)$$

where  $\Gamma \triangleq \{\Gamma_{i,k}^n\}_{n \in \mathcal{O}, i \in \mathcal{B}, k \in \mathcal{U}}$  represents the lower bound of SINR for user  $k$  associated with BS/ST  $i$  over band  $n$ ;  $\beta \triangleq \{\beta_{i,k}^n\}_{n \in \mathcal{O}, i \in \mathcal{B}, k \in \mathcal{U}}$  represents the upper bound of total interference and noise received at user  $k$ ;  $\varphi \triangleq \{\varphi_{i,k}^n\}_{n \in \mathcal{O}, i \in \mathcal{B}, k \in \mathcal{U}}$  represents the upper bound of SINR for user  $k$  associated with BS/ST  $i$  over band  $n$ ;  $\rho \triangleq \{\rho_{i,k}^n\}_{n \in \mathcal{O}, i \in \mathcal{B}, k \in \mathcal{U}}$  represents the lower bound of interference and noise received at user  $k$ .

By introducing  $\Gamma$  and  $\varphi$ , the MBC (12b) and backhaul constraint (13h) can be satisfied at the optimality, respectively. Besides, it is obvious that the constraints from (13c) to (13f) should hold with equality at the optimality. Thus, the equivalence between (12) and (13) is guaranteed.  $\mathbf{P1.1}$  is still challenging to tackle due to the non-convex constraints (13c), (13f) and (13h). To make  $\mathbf{P1.1}$  more tractable, we propose to exploit the SCA method to deal with these non-convex constraints.

Note that the right-hand-side (RHS) of (13c) is a joint convex quadratic-over-linear function with respect to  $\mathbf{w}_{i,k}^n$  and  $\beta_{i,k}^n$ . With this fact, we can use the SCA method to

approximate the RHS of (13c) with a lower bound. The RHS of (13c) can be approximated with the first-order Taylor expression as

$$\frac{|\mathbf{h}_{i,k}^n \mathbf{w}_{i,k}^n|^2}{\beta_{i,k}^n} \geq g_1(\mathbf{w}_{i,k}^n, \beta_{i,k}^n), \quad (14)$$

where  $g_1(\mathbf{w}_{i,k}^n, \beta_{i,k}^n)$  is given in (15) on top of the next page,  $\mathbf{w}_{i,k}^n[\tau-1]$ ,  $\beta_{i,k}^n[\tau-1]$  are the iterative optimization variables obtained in iteration  $\tau-1$ , and  $\mathbf{H}_{i,k}^n \triangleq (\mathbf{h}_{i,k}^n)^H \mathbf{h}_{i,k}^n$ . Note that the RHS of (13f) is also a convex function with respect to  $\mathbf{w}$ , and thus its lower bound can be approximated as

$$\tilde{I}_{i,k}^n + I_{i,k}^n + \sigma_t^2 \geq \sum_{(j,k') \neq (i,k)} g_2(\mathbf{w}_{j,k'}^n) + \sigma_t^2, \quad (17)$$

where  $g_2(\mathbf{w}_{j,k'}^n)$  is given in (16) on top of the next page. The RHS of (13h) is a concave function with respect to  $\varphi_{i,k}^n$  and its upper bound can be obtained as

$$\begin{aligned} \log_2(1 + \varphi_{i,k}^n) &\leq g_3(\varphi_{i,k}^n) \\ &\triangleq \log_2(1 + \varphi_{i,k}^n[\tau-1]) + \frac{\varphi_{i,k}^n - \varphi_{i,k}^n[\tau-1]}{\ln 2(1 + \varphi_{i,k}^n[\tau-1])}. \end{aligned} \quad (18)$$

The LHS of (13h) can be expressed as the difference of concave functions, and its lower bound is as follows:

$$\begin{aligned} C_{\ell,i} &\geq C_{\ell,i}(\mathbf{p}) \\ &\triangleq B_{K_a} t_{\ell,i} \left\{ \log_2 \left( \sum_{\ell'} p_{\ell'} G_T(\theta_{\ell',i}) G_R |f_i|^2 + \sigma_s^2 \right) \right. \\ &\quad \left. - C_{\ell,i}^1 - C_{\ell,i}^2 \right\}, \end{aligned} \quad (19)$$

where  $C_{\ell,i}^1$  and  $C_{\ell,i}^2$  are given by

$$\begin{aligned} C_{\ell,i}^1 &= \log_2 \left( \sum_{\ell' \neq \ell} p_{\ell'} [\tau-1] G_T(\theta_{\ell',i}) G_R |f_i|^2 + \sigma_s^2 \right), \\ C_{\ell,i}^2 &= \sum_{\ell' \neq \ell} \frac{G_T(\theta_{\ell',i}) G_R |f_i|^2}{\ln 2(\sum_{\ell' \neq \ell} p_{\ell'} [\tau-1] G_T(\theta_{\ell',i}) G_R |f_i|^2 + \sigma_s^2)} \\ &\quad \times (p_{\ell'} - p_{\ell'}[\tau-1]). \end{aligned}$$

With approximations (14), (17), (18) and (19), we can obtain the reformulated optimization problem at iteration  $\tau$  of SCA as follows:

$$\mathbf{P1.2} : \max_{\mathbf{p}, \mathbf{t}, \tilde{\mathbf{w}}} \sum_{i \in \mathcal{B}} \sum_{k \in \mathcal{U}} x_{i,k} b_{i,k} r_{i,k} \quad (20a)$$

$$\text{s.t. (13b), (13d), (13e), (13g), (13i),}$$

$$\Gamma_{i,k}^n \leq g_1(\mathbf{w}_{i,k}^n, \beta_{i,k}^n), \quad (20b)$$

$$\rho_{i,k}^n \leq \sum_{(j,k') \neq (i,k)} g_2(\mathbf{w}_{j,k'}^n) + \sigma_t^2, \quad (20c)$$

$$\sum_{n \in \mathcal{O}} \sum_{k \in \mathcal{U}} B_C g_3(\varphi_{i,k}^n) \leq C_{\ell,i}(\mathbf{p}). \quad (20d)$$

For notational simplicity, we denote variables  $\Gamma$ ,  $\beta$ ,  $\varphi$ ,  $\rho$ , and  $\mathbf{w}$  as  $\tilde{\mathbf{w}} = \{\mathbf{w}, \Gamma, \beta, \varphi, \rho\}$ , because those variables all depend on  $\mathbf{w}$ . The problem (20) is still not convex because variables

$\mathbf{p}$ ,  $\mathbf{t}$  and  $\varphi$  are coupled due to the constraint (20d). It can be observed that (20) is convex with respect to either  $\{\mathbf{p}, \tilde{\mathbf{w}}\}$  or  $\{\mathbf{t}, \tilde{\mathbf{w}}\}$ . Based on this observation, the BSM method is adopted to solve (20). Specifically,  $\{\mathbf{p}, \mathbf{t}, \tilde{\mathbf{w}}\}$  can be updated in the following manner: given  $\{\mathbf{t}, \mathbf{x}\}$ , optimize  $\{\mathbf{p}, \tilde{\mathbf{w}}\}$ ; and given  $\{\mathbf{p}, \mathbf{x}\}$ , optimize  $\{\mathbf{t}, \tilde{\mathbf{w}}\}$ .

### B. User Association Optimization for WSRM

When variables  $\{\mathbf{p}, \mathbf{t}, \tilde{\mathbf{w}}\}$  are fixed, (20) is an integer programming problem with respect to  $\mathbf{x}$ , which is challenging to tackle. Therefore, we first relax the binary variable constraint (12h) into  $0 \leq x_{i,k} \leq 1$ . Then, to obtain a high-quality solution for the original integer programming problem, a penalty term  $\varrho(x_{i,k}^2 - x_{i,k})$  is introduced into the objective (20a) to force  $x_{i,k}$  to be binary, where  $\varrho$  is a positive penalty parameter. The reformulated problem is written as follows:

$$\mathbf{P1.3} : \max_{\mathbf{x}} \sum_{i \in \mathcal{B}} \sum_{k \in \mathcal{U}} x_{i,k} b_{i,k} R_{i,k} + \varrho \sum_{i \in \mathcal{B}} \sum_{k \in \mathcal{U}} (x_{i,k}^2 - x_{i,k}) \quad (21a)$$

$$\text{s.t. (12g), (13g), (20d),} \quad (21b)$$

$$0 \leq x_{i,k} \leq 1. \quad (21c)$$

Considering the penalty term is a convex function of  $x_{i,k}$ , we approximate it with the SCA method, which is given by

$$\begin{aligned} (x_{i,k}^2 - x_{i,k}) &\geq f(x_{i,k}) \\ &\triangleq (2x_{i,k}[\tau-1] - 1)x_{i,k} \\ &\quad - x_{i,k}^2[\tau-1], \end{aligned} \quad (22)$$

where  $x_{i,k}[\tau-1]$  is the iterative optimization variable obtained in iteration  $\tau-1$ . With (22), we can write the problem at iteration  $\tau$  of the SCA as

$$\mathbf{P1.4} : \max_{\mathbf{x}} \sum_{i \in \mathcal{B}} \sum_{k \in \mathcal{U}} x_{i,k} b_{i,k} R_{i,k} + \varrho \sum_{i \in \mathcal{B}} \sum_{k \in \mathcal{U}} f(x_{i,k}) \quad (23)$$

$$\text{s.t. (21b), (21c).}$$

**P1.4** is a linear programming problem with respect to  $\mathbf{x}$  and can be easily solved. Besides, it can be verified that, when  $\varrho \rightarrow \infty$ , the solution  $\mathbf{x}$  of **P1.4** will satisfy the binary constraint (12h) [38]. However, if  $\varrho$  is too large, the objective of (23) will be dominated by the penalty term, and the original objective (i.e., WSR) will be diminished. To avoid this, we first initialize  $\varrho$  to a small value to find a good starting point and then gradually increase  $\varrho$  as:  $\varrho = q\varrho$ , where  $q > 1$ . The overall algorithm is summarized in Algorithm 1.

### C. Obtaining Revenue without Inter-operator Sharing

$U_z^0$  can be determined by solving the WSRM problem without inter-operator sharing, which can be formulated as follows

$$\mathbf{P2} : \max_{\mathbf{p}, \mathbf{t}, \tilde{\mathbf{w}}, \mathbf{x}} \sum_{i \in \mathcal{B}_z} \sum_{k \in \mathcal{U}_z} x_{i,k} b_{i,k} R_{i,k} \quad (24a)$$

$$\text{s.t. (12c), (12d), (12f), (12g),}$$

$$\sum_{k \in \mathcal{U}_z} \|\mathbf{w}_{i,k}^z\|^2 \leq P_i, \forall i \in \mathcal{B}_z, \quad (24b)$$

$$x_{i,k} = \begin{cases} 0 \text{ or } 1, & \text{if } i \in \mathcal{B}_z, k \in \mathcal{U}_z, \\ 0, & \text{otherwise,} \end{cases} \quad (24c)$$

$$g_1(\mathbf{w}_{i,k}^n, \beta_{i,k}^n) \triangleq \frac{2\text{Re} \left\{ \left( \mathbf{w}_{i,k}^n[\tau-1] \right)^H \mathbf{H}_{i,k}^n \mathbf{w}_{i,k}^n \right\}}{\beta_{i,k}^n[\tau-1]} - \frac{\left| \mathbf{h}_{i,k}^n \mathbf{w}_{i,k}^n[\tau-1] \right|^2}{\left( \beta_{i,k}^n[\tau-1] \right)^2} \beta_{i,k}^n \quad (15)$$

$$g_2(\mathbf{w}_{j,k'}^n) \triangleq 2\text{Re} \left\{ \left( \mathbf{w}_{j,k'}^n[\tau-1] \right)^H \mathbf{H}_{j,k'}^n \mathbf{w}_{j,k'}^n \right\} - \left| \mathbf{h}_{j,k'}^n \mathbf{w}_{j,k'}^n[\tau-1] \right|^2 \quad (16)$$

---

**Algorithm 1** Centralized Optimization Algorithm for WSRM

- 1: Initialize  $\mathbf{p}[0], \mathbf{t}[0], \tilde{\mathbf{w}}[0], \mathbf{x}[0]$  to feasible values.
  - 2: **repeat**
  - 3:   **repeat**
  - 4:     Update  $\mathbf{p}[\tau], \tilde{\mathbf{w}}[\tau]$  by solving (20) with given  $\mathbf{t}[\tau-1]$  and  $\mathbf{x}[\tau-1]$ .
  - 5:     Update  $\mathbf{t}[\tau], \tilde{\mathbf{w}}[\tau]$  by solving (20) with given  $\mathbf{p}[\tau]$  and  $\mathbf{x}[\tau-1]$ .
  - 6:     Update  $\mathbf{x}[\tau]$  by solving (23) with given  $\mathbf{p}[\tau], \mathbf{t}[\tau]$  and  $\tilde{\mathbf{w}}[\tau]$ .
  - 7:   **until** The objective converges or the maximum number of iterations is reached.
  - 8:    $\varrho = q\varrho$ .
  - 9: **until**  $f(x_{i,k})$  is below a certain threshold  $\epsilon$  or the maximum number of iterations is reached.
- 

where (24b) indicates there is no spectrum sharing, and (24c) indicates that each user can only be associated with the BSs/STs of the same operator. Further,  $R_{i,k}$  in (24a) is given by

$$R_{i,k} = \log_2(1 + \gamma_{i,k}^n), \quad (25)$$

where  $\gamma_{i,k}^n$  can be obtained by (7) with  $I_{i,k}^n = 0$ . **P2** can be decomposed into independent subproblems for different operators. Similar to **P1**, the subproblem for operator  $n$  can be equivalently reformulated as

$$\begin{aligned} \mathbf{P2.1} : \max_{\mathbf{p}, \mathbf{t}, \tilde{\mathbf{w}}, \mathbf{x}} \sum_{i \in \mathcal{B}_z} \sum_{k \in \mathcal{U}_z} x_{i,k} b_{i,k} r_{i,k} \\ \text{s.t. (12c), (12f), (12g), (24b), (24c),} \\ (20b) - (20d), \end{aligned} \quad (26)$$

It is clear that **P2.1** can be regarded as a special case of **P1.2**. Therefore, the algorithm proposed for **P1.2** can be applied to solving **P2.1**. Different from **P1.2**, MBCs are not considered in **P2.1**, and there exists optimal  $\mathbf{x}$  of **P2.1** are binary variables. Hence, we do not need to introduce the penalty term (22) to the objective of (26). If we solve  $\mathbf{x}$  directly to the global optimality,  $\mathbf{x}$  will not change during the algorithm and fix at 0 or 1. To find a good  $\mathbf{x}$ , we exploit the gradient projection [39] for updating  $\mathbf{x}$ , which is given by

$$x_{i,k} = P_{\Omega_x} (x_{i,k} + \eta b_{i,k} R_{i,k}), \quad (27)$$

where  $P_{\Omega_x}(\cdot)$  is the projection to the set  $\Omega_x = \{x_{i,k} \mid (12g), (24c)\}$ , and  $\eta$  is the step size. The overall algorithm is summarized in Algorithm 2.

#### D. Finding Initial Points

The feasible initial points are important for the SCA-based algorithm. However, due to the backhaul constraint (20d) and

---

**Algorithm 2** Algorithm for Obtaining Revenue without Inter-operator Sharing

- 1: Initialize  $\mathbf{p}[0], \mathbf{t}[0], \tilde{\mathbf{w}}[0], \mathbf{x}[0]$  to feasible values.
  - 2: **repeat**
  - 3:   Update  $\mathbf{p}[\tau], \tilde{\mathbf{w}}[\tau]$  by solving (26) with given  $\mathbf{t}[\tau-1]$  and  $\mathbf{x}[\tau-1]$ .
  - 4:   Update  $\mathbf{t}[\tau], \tilde{\mathbf{w}}[\tau]$  by solving (26) with given  $\mathbf{p}[\tau]$  and  $\mathbf{x}[\tau-1]$ .
  - 5:   Update  $\mathbf{x}$  with the gradient projection method (27) with given  $\mathbf{p}[\tau], \mathbf{t}[\tau]$  and  $\tilde{\mathbf{w}}[\tau]$ .
  - 6: **until** The objective converges or the maximum number of iterations is reached.
- 

MBC (13g), it is challenging to find feasible initial points for **P1.2**. To address this issue, we propose a penalty method to find the feasible initial points [40]. Specifically, we can obtain initial points by solving the following optimization problem

$$\mathbf{P3} : \max_{\mathbf{p}, \mathbf{t}, \tilde{\mathbf{w}}, \mathbf{x}, \mathbf{s}} \sum_{i \in \mathcal{B}} \sum_{k \in \mathcal{U}} x_{i,k} b_{i,k} r_{i,k} - \xi \left( \sum_{z \in \mathcal{O}} s_{u_z} + \sum_{i \in \mathcal{B}_S} s_{b_i} \right) \quad (28a)$$

s.t. (13b), (13d), (13e), (13i), (20b)

$$\sum_{i \in \mathcal{B}} \sum_{k \in \mathcal{U}} x_{i,k} \alpha_{i,k}^z r_{i,k} + s_{u_z} \geq U_z^0, \quad (28b)$$

$$\sum_{n \in \mathcal{O}} \sum_{k \in \mathcal{U}} B_C g_3(\varphi_{i,k}^n) \leq C_{\ell,i}(\mathbf{p}) + s_{b_i}, \quad (28c)$$

$$s_{u_z}, s_{b_i} \geq 0, \quad (28d)$$

where  $\xi$  is a positive penalty parameter and  $\mathbf{s} \triangleq \{s_{u_z}, s_{b_i}\}_{z \in \mathcal{O}, i \in \mathcal{B}_S}$  are slack variables. The basic idea of the above formulation is forcing the penalty terms to be zero by maximizing (28a). **P3** can also be solved with the BSM method. Besides, the gradient projection can be exploited for updating  $\mathbf{x}$  and  $\mathbf{s}$ , which is given by

$$(x_{i,k}, s_{u_z}) = P_{\Omega_{x,s}} (x_{i,k} + \eta b_{i,k} R_{i,k}, s_{u_z} - \eta \xi), \quad (29)$$

where  $P_{\Omega_{x,s}}(\cdot)$  is the projection to the set  $\Omega_{x,s} = \{x_{i,k}, s_{u_z} \mid (12g), (13g), (21c)\}$ . The overall algorithm is summarized in Algorithm 3.

#### E. Convergence and Complexity Analysis

Algorithms proposed in this section have similar main process. As a result, we mainly analyze the convergence and complexity of Algorithm 1, and the results can be applied to Algorithm 2 and 3. The convergence of Algorithm 1 is provided as follows.

**Proposition 1.** *Algorithm 1 is guaranteed to converge*

*Proof.* Please refer to Appendix A □

---

**Algorithm 3** Initial Points Searching Algorithm

---

- 1: Initialize  $\mathbf{p}[0], \mathbf{t}[0], \tilde{\mathbf{w}}[0], \mathbf{x}[0]$  to feasible values.
  - 2: **repeat**
  - 3: Update  $\mathbf{p}[\tau], \tilde{\mathbf{w}}[\tau], \mathbf{s}$  by solving (28) with given  $\mathbf{t}[\tau-1]$  and  $\mathbf{x}$ .
  - 4: Update  $\mathbf{t}[\tau], \tilde{\mathbf{w}}[\tau], \mathbf{s}$  by solving (28) with given  $\mathbf{p}[\tau-1]$  and  $\mathbf{x}$ .
  - 5: Update  $\mathbf{x}, \mathbf{s}$  using gradient projection (29) with given  $\mathbf{p}[\tau], \mathbf{t}[\tau]$  and  $\tilde{\mathbf{w}}[\tau]$ .
  - 6: **until**  $\|\mathbf{s}\|_\infty$  is below a certain threshold  $\epsilon$  or the maximum number of iterations is reached.
- 

The main complexity of Algorithm 1 is caused by solving (20) and (23) in the inner loop. The worst-case complexity of Algorithm 1 depends on the number of variables, which can be upper bound as

$$\mathcal{O}\{I_{out}^1 I_{in}^1 ((N_L + N_t(N_B + N'_B))(N_U + N'_U))^4 + (N'_B + N_t(N_B + N'_B))(N_U + N'_U))^4 + ((N_B + N'_B)(N_U + N'_U))^4\}$$

where  $I_{out}^1$  and  $I_{in}^1$  are the number of outer and inner iterations, respectively.

## V. DISTRIBUTED ALGORITHMS FOR WSRM

The centralized algorithm proposed in Section IV is challenging to implement in the real SAGIN. In this section, we propose a distributed algorithm for the WSRM problem, which can be implemented in local centers independently. Specifically, we develop a distributed user association algorithm based on the Lagrangian dual decomposition and a distributed algorithm for beamforming design and resource allocation based on the consensus ADMM.

### A. Lagrangian Dual Decomposition-based User Association Design

With fixed  $\{\mathbf{p}, \mathbf{t}, \tilde{\mathbf{w}}\}$ , **P1.1** can be reformulated as

$$\mathbf{P1.5} : \max_{\mathbf{x}} \sum_{i \in \mathcal{B}} \sum_{k \in \mathcal{U}} x_{i,k} b_{i,k} R_{i,k} \quad (30a)$$

$$\text{s.t. (12b), (12g), (12h),} \quad (30b)$$

It is clear that **P1.5** is non-convex due to the binary variables  $\mathbf{x}$ . Although the centralized algorithm can tackle this problem efficiently by relaxing binary variables, it is difficult to implement in the real SAGIN due to high complexity. Keeping that in mind, we propose a distributed user association algorithm based on the Lagrangian dual decomposition [41], [42].

First, the Lagrangian function with respect to constraint (12b) is

$$L(\mathbf{x}, \boldsymbol{\lambda}) = \sum_{i \in \mathcal{B}} \sum_{k \in \mathcal{U}} x_{i,k} b_{i,k} R_{i,k} + \sum_{z \in \mathcal{O}} \lambda_z (U_z - U_z^0), \quad (31)$$

where  $\boldsymbol{\lambda}$  are dual variables introduced for (12b). Then the dual function is given as

$$g(\boldsymbol{\lambda}) = \begin{cases} \max_{\mathbf{x}} L(\mathbf{x}, \boldsymbol{\lambda}) \\ \text{s.t. (12g), (12h)} \end{cases}. \quad (32)$$

Based on the dual function, the Lagrange dual problem of **P1.5** can be written as

$$\min_{\boldsymbol{\lambda}} g(\boldsymbol{\lambda}). \quad (33)$$

Now, the solution to **P1.5** can be obtained by solving (33). Note that since **P1.5** is non-convex and discrete in nature, solving (33) is not equivalent to solving **P1.5**, and there may exist a duality gap. Nevertheless, good primal solutions can often be obtained by solving the dual problem [42].

Compared with **P1.3**, (33) can be decomposed into independent subproblems for each user and BS/ST and then solved in a distributed manner. Specifically, (33) can be solved in two levels, i.e., the inner maximization problem at the user level and the outer minimization problem at the operator level. In the inner layer,  $\mathbf{x}$  is optimized to maximize the Lagrangian function (31) with given  $\boldsymbol{\lambda}$ . The maximization of the Lagrangian function (31) has the following explicit analytic solution:

$$x_{ik}^* = \begin{cases} 1, & \text{if } i = \arg \max_j (b_{j,k} + \sum_z \lambda_z \alpha_{j,k}^z) R_{j,k} \\ 0, & \text{otherwise.} \end{cases} \quad (34)$$

We can see that optimal  $x_{ik}^*$  can be determined by each user  $k$  independently according to (34). On the other hand, the dual problem (33) is convex concerning  $\boldsymbol{\lambda}$  and thus can be solved with the subgradient method. With  $x_{ik}^*$ , the dual variables can be updated as

$$\lambda_z = [\lambda_z - \eta (U_z - U_z^0)]^+, \quad (35)$$

where  $x^+ = \max\{x, 0\}$ . Specifically,  $\boldsymbol{\lambda}$  can be updated by each operator independently. The above algorithm is compactly written in Algorithm 4

---

**Algorithm 4** Distributed Algorithm for User Association

---

- 1: Initialize  $\mathbf{x}, \boldsymbol{\lambda}$  to feasible values.
  - 2: **repeat**
  - 3: Each user updates  $\mathbf{x}$  according to (34).
  - 4: Each operator updates  $\boldsymbol{\lambda}$  according to (35) and broadcasts  $\boldsymbol{\lambda}$  to all users.
  - 5: **until** The dual objective converges or the maximum number of iterations is reached.
- 

### B. Consensus ADMM-based Resource Allocation and Beamforming Design

Due to the inter-operator interference (8b) and the MBC (12b), Algorithm 1 is required to be implemented in a centralized manner, which is challenging to realize in practice. To this end, we propose an algorithm based on the consensus ADMM [43] to tackle this problem distributedly.

First, **P1.2** can be equivalently rewritten as follows:

$$\mathbf{P1.2.1} : \max_{\substack{\mathbf{p}, \mathbf{t}, \tilde{\mathbf{w}}, \\ \Gamma, \hat{\theta}, \hat{\psi}}} \sum_{z \in \mathcal{O}} \sum_{i \in \mathcal{B}_z} \sum_{k \in \mathcal{U}} x_{i,k} b_{i,k} r_{i,k}^{(z)} \quad (36a)$$

$$\text{s.t. (13b), (13e), (20d),}$$

$$r_{i,k}^{(z)} = \sum_{n \in \mathcal{O}} \log_2(1 + \Gamma_{i,k}^{n,(z)}), \quad (36b)$$

$$\sum_{i \in \mathcal{B}_z} \sum_{k \in \mathcal{U}} x_{i,k} \alpha_{i,k}^z r_{i,k}^{(z)} \geq U_z^0, \quad (36c)$$

$$\Gamma_{i,k}^{n,(z)} \leq g_1(\mathbf{w}_{i,k}^n, \beta_{i,k}^n), \quad (36d)$$



$$\rho_{i,k}^n \geq \tilde{I}_{i,k}^n + \sum_{m \in \mathcal{O} \setminus \{z\}} \theta_{m,k}^{n,(z)} + \sigma_t^2, \quad (36e)$$

$$\rho_{i,k}^n \leq \sum_{i \in \mathcal{B}_z} \sum_{k' \in \mathcal{U} \setminus \{k\}} g_2(\mathbf{w}_{i,k'}^n) + \sum_{m \in \mathcal{O} \setminus \{z\}} \psi_{m,k}^{n,(z)}, \quad (36f)$$

$$\theta_{z,k}^{n,(z)} \geq \sum_{i \in \mathcal{B}_z} \sum_{k' \in \mathcal{U} \setminus \{k\}} |\mathbf{h}_{i,k}^n \mathbf{w}_{i,k'}^n|^2, \quad (36g)$$

$$\psi_{z,k}^{n,(z)} \leq \sum_{i \in \mathcal{B}_z} \sum_{k' \in \mathcal{U} \setminus \{k\}} g_2(\mathbf{w}_{i,k'}^n), \quad (36h)$$

$$\Gamma_{i,k}^{n,(z)} = \tilde{\Gamma}_{i,k}^n, \quad (36i)$$

$$\theta_{z,k}^{n,(m)} = \hat{\theta}_{z,k}^n, \quad (36j)$$

$$\psi_{z,k}^{n,(m)} = \hat{\psi}_{z,k}^n, \quad (36k)$$

where  $\bar{\mathbf{w}} \triangleq \{\bar{\mathbf{w}}_z\}_{z \in \mathcal{O}}$ , and  $\bar{\mathbf{w}}_z \triangleq \{\mathbf{w}_{i,k}^n, \beta_{i,k}^n, \varphi_{i,k}^n, \rho_{i,k}^n, \Gamma_{i,k}^{n,(z)}, \theta_{i,k}^{n,(z)}, \psi_{i,k}^{n,(z)}\}_{n \in \mathcal{O}, i \in \mathcal{B}_z, k \in \mathcal{U}}$  represents the local variables of operator  $z$ .  $\Gamma_{i,k}^{n,(z)}$ ,  $\theta_{i,k}^{n,(z)}$  and  $\psi_{i,k}^{n,(z)}$  are newly introduced slack variables. Specifically,  $\Gamma_{i,k}^{n,(z)}$  represents the SINR of user  $k$  associated with BS/ST  $i$  over band  $n$ , while  $\theta_{i,k}^{n,(z)}$  and  $\psi_{i,k}^{n,(z)}$  denote the upper and lower bound for the inter-operator interference that operator  $z$  causes to user  $k$  over band  $n$ , respectively. The reason we introduce  $\theta_{i,k}^{n,(z)}$  is to guarantee MBCs (36c), while that for  $\psi_{i,k}^{n,(z)}$  is to satisfy backhaul constraints (20d).

Note that  $\Gamma_{i,k}^{n,(z)}$ ,  $\theta_{i,k}^{n,(z)}$  and  $\psi_{i,k}^{n,(z)}$  are all obtained and optimized by operator  $z$  locally. Intuitively,  $\Gamma_{i,k}^{n,(z)}$  is a local version of  $\Gamma_{i,k}^n$  determined by operator  $z$ , while  $\theta_{i,k}^{n,(z)}$  and  $\psi_{i,k}^{n,(z)}$  are the local versions of  $I_{j,k}^n, j \in \mathcal{B} \setminus \mathcal{B}_z$ . On the other hand,  $\dot{\Gamma} \triangleq \{\dot{\Gamma}_{i,k}^n\}$ ,  $\dot{\theta}_{i,k}^n \triangleq \{\dot{\theta}_{i,k}^n\}$  and  $\dot{\psi}_{i,k}^n \triangleq \{\dot{\psi}_{i,k}^n\}$  are the corresponding global versions of  $\Gamma_{i,k}^n$ ,  $\theta_{i,k}^n$  and  $\psi_{i,k}^n$ , which can be obtained through aggregating local variables across operators. The constraints (36i)-(36k) can make sure that operators finally reach a consensus on the value of SINR and inter-operator interference, guaranteeing the equivalence of (20) and (36).

With the introduced slack variables, the constraints from (36c) to (36h) can be decomposed into independent local convex sets for each operator, and the local set for operator  $z$  is:

$$\mathcal{C}_z = \left\{ (\mathbf{p}, \mathbf{t}, \bar{\mathbf{w}}_z) \mid (13b), (13e), (20d), (36b) - (36h) \right\}, \quad (37)$$

Then, the subproblem of (36) for operator  $z$  can be compactly expressed as

$$\text{P1.2.2: } \min_{\substack{\mathbf{p}, \mathbf{t}, \bar{\mathbf{w}}_z \\ \dot{\Gamma}, \dot{\theta}, \dot{\psi}}} \sum_{i \in \mathcal{B}_z} \sum_{k \in \mathcal{U}} -x_{i,k} b_{i,k} r_{i,k}^{(z)} \quad (38a)$$

s.t. (36b)

$$(\mathbf{p}, \mathbf{t}, \bar{\mathbf{w}}_z) \in \mathcal{C}_z, \quad (38b)$$

$$\Gamma_{i,k}^{n,(z)} = \dot{\Gamma}_{i,k}^n, \forall i \in \mathcal{B}, \forall k \in \mathcal{U}, \quad (38c)$$

$$\theta_{z,k}^{n,(m)} = \dot{\theta}_{z,k}^n, \forall m \in \mathcal{O}, \forall i \in \mathcal{B}, \forall k \in \mathcal{U}, \quad (38d)$$

$$\psi_{z,k}^{n,(m)} = \dot{\psi}_{z,k}^n, \forall m \in \mathcal{O}, \forall i \in \mathcal{B}, \forall k \in \mathcal{U}. \quad (38e)$$

For notational simplicity, define  $\Phi_z \triangleq \{\mathbf{p}, \mathbf{t}, \bar{\mathbf{w}}_z\}$  and  $F_z \triangleq \{\Gamma_{i,k}^{n,(z)}\}_{n \in \mathcal{O}, i \in \mathcal{B}_z, k \in \mathcal{U}}$ . Similarly, we define  $\theta_z$  and  $\psi_z$ . Then the augmented Lagrangian of (38) can be written in the following

$$\begin{aligned} L(\Phi_z, \dot{\Gamma}, \dot{\theta}, \dot{\psi}, \nu_z) &= \sum_{i \in \mathcal{B}_z} \sum_{k \in \mathcal{U}} -x_{i,k} b_{i,k} r_{i,k}^{(z)} + \mathbb{I}_{\mathcal{C}_z}(\Phi_z) \\ &+ \nu_{z,\Gamma}^T (F_z - \dot{\Gamma}) + \frac{c}{2} \|F_z - \dot{\Gamma}\|^2 \\ &+ \nu_{z,\theta}^T (\theta_z - \dot{\theta}) + \frac{c}{2} \|\theta_z - \dot{\theta}\|^2 \\ &+ \nu_{z,\psi}^T (\psi_z - \dot{\psi}) + \frac{c}{2} \|\psi_z - \dot{\psi}\|^2, \end{aligned}$$

where  $\mathbb{I}_{\mathcal{C}_z}(\Phi_z)$  is an indicator function defined as

$$\mathbb{I}_{\mathcal{C}_z}(\Phi_z) = \begin{cases} 0, & \text{if } \Phi_z \in \mathcal{C}_z, \\ +\infty, & \text{otherwise,} \end{cases}$$

$\nu_z \triangleq \{\nu_{z,\Gamma}, \nu_{z,\theta}, \nu_{z,\psi}\}$  denotes the dual variables related to constraints (38c)-(38e) of operator  $z$ , and  $c$  is the penalty coefficient introduced for penalizing the violation of equality constraints.

In the following, we elaborate on the variable updates in ADMM. First, the local variables  $\{\mathbf{p}, \bar{\mathbf{w}}_z\}$  or  $\{\mathbf{t}, \bar{\mathbf{w}}_z\}$  in the  $(l+1)$ -th iteration can be updated as follows:

$$\begin{aligned} (\mathbf{p}, \bar{\mathbf{w}}_z)^{(l+1)} &= \arg \min_{\mathbf{p}, \bar{\mathbf{w}}_z} L(\Phi^{(l)}, \dot{\Gamma}^{(l)}, \dot{\theta}^{(l)}, \dot{\psi}^{(l)}, \nu_z^{(l)}), \\ (\mathbf{t}, \bar{\mathbf{w}}_z)^{(l+1)} &= \arg \min_{\mathbf{p}, \bar{\mathbf{w}}_z} L(\Phi^{(l)}, \dot{\Gamma}^{(l)}, \dot{\theta}^{(l)}, \dot{\psi}^{(l)}, \nu_z^{(l)}). \end{aligned} \quad (40)$$

Next, the global variables can be updated as

$$\begin{aligned} \dot{\Gamma}^{(l+1)} &= \frac{1}{|\mathcal{O}|} \sum_{z \in \mathcal{O}} \left( F_z^{(l+1)} + \frac{1}{c} \nu_{z,\Gamma}^{(l)} \right), \\ \dot{\theta}^{(l+1)} &= \frac{1}{|\mathcal{O}|} \sum_{z \in \mathcal{O}} \left( \theta_z^{(l+1)} + \frac{1}{c} \nu_{z,\theta}^{(l)} \right), \\ \dot{\psi}^{(l+1)} &= \frac{1}{|\mathcal{O}|} \sum_{z \in \mathcal{O}} \left( \psi_z^{(l+1)} + \frac{1}{c} \nu_{z,\psi}^{(l)} \right), \end{aligned} \quad (41)$$

where  $|\mathcal{O}|$  is the number of operators. Finally, dual variables can be updated as follows:

$$\begin{aligned} \nu_{z,\Gamma}^{(l+1)} &= \nu_{z,\Gamma}^{(l)} + c(F_z^{(l+1)} - \dot{\Gamma}^{(l+1)}), \\ \nu_{z,\theta}^{(l+1)} &= \nu_{z,\theta}^{(l)} + c(\theta_z^{(l+1)} - \dot{\theta}^{(l+1)}), \\ \nu_{z,\psi}^{(l+1)} &= \nu_{z,\psi}^{(l)} + c(\psi_z^{(l+1)} - \dot{\psi}^{(l+1)}). \end{aligned} \quad (42)$$

The algorithm for updating  $\{\mathbf{p}[\tau], \bar{\mathbf{w}}[\tau]\}$  or  $\{\mathbf{t}[\tau], \bar{\mathbf{w}}[\tau]\}$  is summarized in Algorithm 5.

Motivated by the fact observed in [44], we adopt the early termination strategy in the ADMM-loop. However, the new objective value may be worse than the previous one due to limited iterations. In this case, we will increase  $I_{ADMM}$  and not accept the new results. The overall algorithm is summarized in Algorithm 6.

### C. Convergence and Complexity Analysis

The convergence of Algorithm 6 is provided as follows.

**Proposition 2.** *Algorithm 6 is guaranteed to converge.*

*Proof.* Please refer to Appendix B □

### Algorithm 5 Distributed Algorithm for Resource Allocation and Beamforming

- 1: Input  $\mathbf{p}[\tau - 1], \mathbf{t}[\tau - 1], \bar{\mathbf{w}}[\tau - 1], \mathbf{x}[\tau - 1], \nu_z$ .
- 2: **repeat**
- 3: Each operator updates local variables  $\{\mathbf{p}[\tau], \bar{\mathbf{w}}_z[\tau]\}$  or  $\{\mathbf{t}[\tau], \bar{\mathbf{w}}_z[\tau]\}$  according to (40).
- 4: Each operator shares  $\Gamma_z, \theta_z$  and  $\psi_z$  with each other and updates global variables  $\hat{\Gamma}, \hat{\theta}$  and  $\hat{\psi}$  according to (41).
- 5: Each operator updates dual variables  $\nu_z$  according to (42).
- 6: **until** The objective converges or the maximum number of iterations is reached.
- 7: **if** The new WSR is smaller than the previous one **then**
- 8: Increase the maximum number of ADMM iteration  $I_{ADMM}$
- 9: Return  $\{\mathbf{p}[\tau - 1], \bar{\mathbf{w}}[\tau - 1]\}$  or  $\{\mathbf{t}[\tau - 1], \bar{\mathbf{w}}[\tau - 1]\}$
- 10: **end if**

### Algorithm 6 Distributed Algorithm for WSRM

- 1: Initialize  $\mathbf{p}[0], \mathbf{t}[0], \bar{\mathbf{w}}[0], \mathbf{x}[0]$  to feasible values.
- 2: **repeat**
- 3: Update  $\mathbf{p}[\tau], \bar{\mathbf{w}}[\tau]$  via Algorithm 5.
- 4: Update  $\mathbf{t}[\tau], \bar{\mathbf{w}}[\tau]$  via Algorithm 5.
- 5: Update  $\mathbf{x}$  via Algorithm 4.
- 6: **until** The objective converges or the maximum number of iterations is reached.

The complexity of Algorithm 6 is dominated by Algorithm 4 (line 5 of Algorithm 6) and Algorithm 5 (line 3 and 4 of Algorithm 6). The complexity of Algorithm 4 is  $\mathcal{O}(I_{UA}(N_B + N'_B)(N_U + N'_U))$ , in which  $I_{UA}$  is the iteration number of Algorithm 4. The main complexity of Algorithm 5 is solving (40), which is similar to Algorithm 1. As a result, the complexities for line 3 and 4 of Algorithm 6 are  $\mathcal{O}(I_{ADMM}(N_L + (N_B + N'_B)(N_U + N'_U))^4)$  and  $\mathcal{O}(I_{ADMM}(N'_B + (N_B + N'_B)(N_U + N'_U))^4)$ , respectively.

## VI. SIMULATION RESULTS

In this section, simulation results are provided to demonstrate the effectiveness of the proposed algorithms and the significance of the MBCs. The considered SAGIN is shown in Fig. 2. Specifically, GNO has  $N_B = 2$  BSs and  $N_U = 3$  users, while SNO has  $N'_B = 4$  STs and  $N'_U = 7$  users. Each BS/ST is equipped with  $N_t = 4$  antennas, and the maximum transmit power for each BS is 52 dBm, and for each ST, it is 49 dBm. Besides, we assume each operator has a  $B_C = 100$  MHz dedicated C band. The parameters of the satellite-ground link are summarized in Table II. The channel for the ground-ground link is set as follows: the path-loss is modeled as  $32.4 + 20 \log(f_C) + 30 \log(d)$ , where  $f_C = 3$  is the carrier frequency in GHz and  $d$  is the distance in km. The Rayleigh fading is adopted to characterize the small-scale fading, and the noise power spectral density is  $-174$  dBm/Hz. Other parameters are set as follows:  $\rho = 1 \times 10^{-4}$ ,  $q = 50$ ,  $\epsilon = 20$ ,  $\eta = 0.1$ ,  $\epsilon = 10^{-3}$ ,  $c = 1.5$ , and  $b_{i,k} = 1, \forall i, k$ .

To show the effectiveness of the proposed algorithms, we consider the following baseline algorithms for comparison.

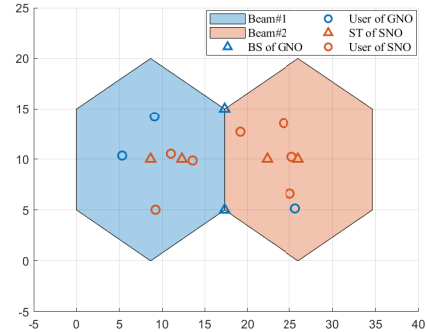


Fig. 2. The considered SAGIN.

TABLE II  
SYSTEM PARAMETERS FOR SATELLITE-GROUND LINK

PARAMETER	VALUE
LEO height	600 km
The number of beams	$N_L = 2$
Beam radius	10 km
Carrier frequency	$f_{Ka} = 20$ GHz
System bandwidth	$B_{Ka} = 400$ MHz
LEO maximum transmit power	$P_{Sat} = 50$ W
LEO maximum transmit gain	$G_T^0 = 40$ dBi
LEO antenna aperture	0.6 m
ST maximum receive gain	$G_R = 10$ dBi
ST antenna temperature	150 K
Environment temperature	290 K
Boltzmann constant	$1.38 \times 10^{-23}$ J/K
Noise figure	1.2 dB
Path-loss	$92.44 + 20 \log(f_{Ka}) + 20 \log(d)$
SR fading ( $b, m, \Omega$ )	(0.126, 10.1, 0.835)

- **Closest Association and Equal Resource Allocation (CA-ERA):** Each user is connected to the closest BS/ST, with equal power allocation and maximum ratio transmit (MRT) beamforming employed by BSs/STs. The LEO satellite equally allocates power to beams and time to STs within a beam.
- **Closest Association and Optimized Power and Beamforming (CA-OPW):** The power allocation of the LEO satellite and the beamforming of BSs/STs are optimized with the proposed algorithm.
- **Closest Association and Optimized Time and Beamforming (CA-OTW):** The time allocation of each beam and the beamforming of BSs/STs are optimized with the proposed algorithm.

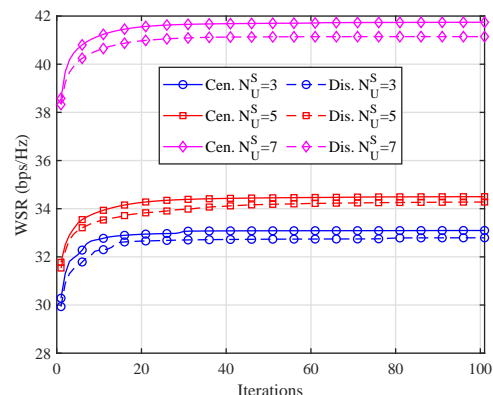


Fig. 3. The convergence of the centralized Algorithm 1 and distributed Algorithm 6:  $\delta_G = \delta_S = 0.6$ .

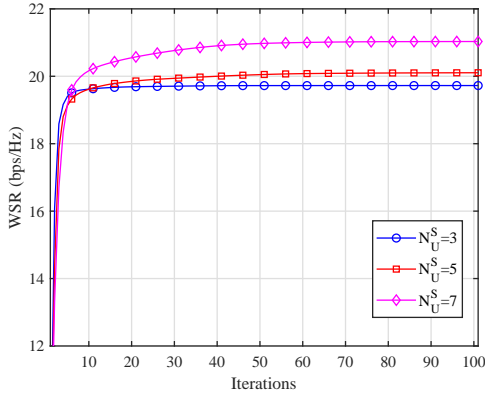


Fig. 4. The convergence of Algorithm 2:  $\delta_G = \delta_S = 0.6$ .

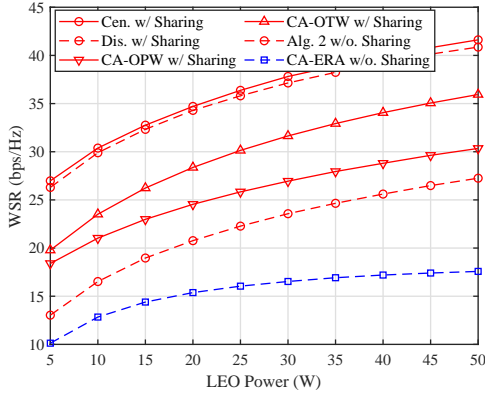


Fig. 5. WSR versus maximum transmit power of the LEO satellite  $P_{Sat}$ :  $\delta_G = \delta_S = 0.6$ ,  $P_i = 52$  dBm,  $i \in \mathcal{B}_G$ ,  $P_j = 49$  dBm,  $j \in \mathcal{B}_S$ .

Firstly, we validate the convergence of proposed Algorithms. In Fig. 3, we show the convergence of the proposed centralized Algorithm 1 ('Cen.') and distributed Algorithm 6 ('Dis.') when  $\delta_G = \delta_S = 0.6$ . It can be seen that both algorithms converge finally, and the distributed algorithm achieves a very close performance to the centralized algorithm. Then, the convergence of the Algorithm 2 is demonstrated in Fig. 4.

Secondly, we compare WSRs achieved by different approaches versus the transmit power of the LEO satellite in Fig. 5. It is clear that WSRs increase with  $P_{Sat}$  increasing, indicating that the impact of backhaul capacity on the WSR. Then, we compare WSRs achieved by Algorithm 2 and CA-ERA for the case without inter-operator sharing ('w/o. Sharing').

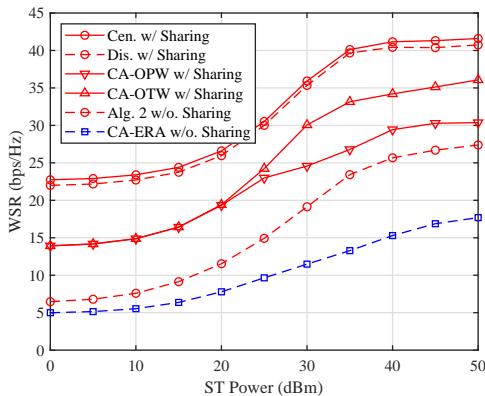


Fig. 6. WSR versus maximum transmit power of STs  $P_i$ ,  $i \in \mathcal{B}_S$ :  $\delta_G = \delta_S = 0.6$ ,  $P_{Sat} = 50$  W.

The proposed algorithm outperforms CR-ERA, demonstrating the effectiveness of Algorithm 2. Besides, we illustrate the WSRs for different approaches in the case with inter-operator sharing ('w/ Sharing'). The distributed algorithm approaches the centralized algorithm and performs much better than other benchmarks. This points out that the necessity of jointly optimizing user association, resource allocation and beamforming design. Moreover, the WSR achieved in the case with inter-operator sharing is much higher than that in the case without inter-operator sharing, indicating significant gains introduced by realizing SAGIN with inter-operator sharing.

Thirdly, we investigate the WSRs achieved by different approaches versus the transmit power of STs in Fig. 6. It can be seen that the WSR in the case with inter-operator sharing does not keep increasing as  $P_i$  increases. Particularly, when  $P_i$  is greater than 40 dBm, the WSR almost remains the same. This indicates that the backhaul capacity provided by the LEO satellite limits the WSR, which is consistent with the result obtained from Fig. 5. Additionally, by comparing WSRs achieved by different approaches in two cases, we can find that the proposed algorithms always realize the highest WSRs and the distributed algorithm performs close to that of the ce

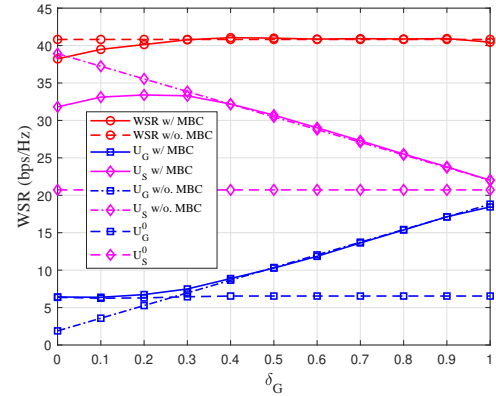


Fig. 7. WSR and operators' revenue versus sharing coefficient of GNO  $\delta_G$ :  $\delta_S = 1$ .

Next, we present the WSR and operators' revenue versus sharing coefficients to investigate the effect of MBCs in Fig. 7 and Fig. 8. Specifically, we consider two cases: i) the symbiotic case with MBCs ('w/ MBC'), and ii) the non-symbiotic case without MBCs ('w/o. MBC'). In Fig. 7, we demonstrate WSRs

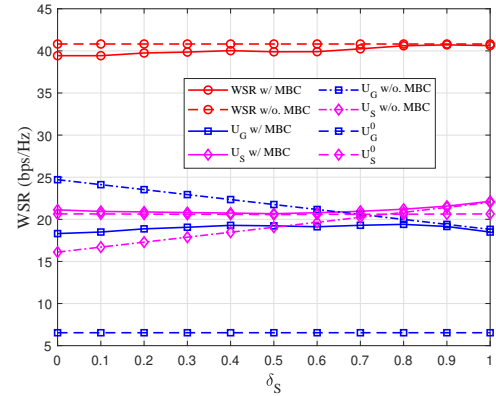


Fig. 8. WSR and operators' revenue versus sharing coefficient of SNO  $\delta_S$ :  $\delta_G = 1$ .

and revenue versus  $\delta_G$  with  $\delta_S = 1$ . By comparing revenue in the two cases, we can find that each operator's revenue in the symbiotic case does not experience revenue loss after sharing spectrum and services. On the contrary, the GNO suffers revenue loss in the non-symbiotic case when  $\delta_G$  is less than 0.2. This indicates that MBCs can enable operators to achieve mutual benefits. Then, we compare the WSRs in the two cases. The WSRs in the symbiotic case are less than those in the non-symbiotic case when  $\delta_G < 0.2$ . The reason is that when  $\delta_G < 0.2$ , the spectrum and service configuration maximizing the WSR makes GNO suffer revenue loss. Therefore, the GNO does not adopt this configuration in the symbiotic case. It is worth noting that the WSRs achieved in the symbiotic case are close to those in the non-symbiotic case when  $\delta_G > 0.2$ , which demonstrates the proposed algorithms can efficiently maximize WSR and achieve mutual benefits. Besides, the WSR and revenue of GNO both grow gradually as  $\delta_G$  increases, while the revenue of the SNO increases first and then decreases when  $\delta_G > 0.3$ . This trend can be explained as follows. With  $\delta_G$  increasing, the GNO can obtain more revenue from serving users of SNO. As a result, the GNO demonstrates a growing preference for inter-operator sharing, increasing the WSR and revenue of operators. However when  $\delta_G > 0.3$ , the GNO takes away the most revenue from serving SNO's users, resulting in revenue loss of SNO.

Lastly, we study the WSR and revenue versus the sharing coefficient of SNO  $\delta_S$  in Fig. 8. It can be seen that the MBC for SNO cannot be satisfied until  $\delta_S \geq 0.8$  in the non-symbiotic case. Besides, the WSR and revenue in the symbiotic case almost remain the same when  $\delta_S < 0.8$ . The reason is that the SNO cannot benefit enough from inter-operator sharing and lacks the motivation to share spectrum and services. On the other hand, by comparing Fig. 7 and Fig. 8, it can be observed that the GNO will obtain benefit when ( $\delta_G \geq 0.3, \delta_S = 1$ ) while the SNO gains when ( $\delta_S \geq 0.8, \delta_G = 1$ ). This result indicates a principle to achieve mutual benefits when inter-operator sharing is enabled: the operator with more resources, like the SNO in this paper, should get more compensation from others. On the contrary, the GNO, who contributes less to the SAGIN, should not require much compensation from others.

## VII. CONCLUSION

In this paper, we have studied a SAGIN consisting of a GNO and SNO, and inter-operator sharing has been adopted to construct such a large-scale network. To fully leverage the advantage of inter-operator sharing, both system performance and individual benefits should be considered. Therefore, we have investigated the spectrum and service sharing in the SAGIN from a symbiotic communication perspective, which can instruct different operators to achieve mutual benefits. Specifically, we have studied a WSR maximization problem about jointly optimizing the user association, resource allocation, and beamforming design. Besides, we have introduced a sharing coefficient to characterize the revenue of each operator, based on which the MBC has been formulated to guarantee that revenue for all operators does not decline after inter-operator

sharing. Then, we have proposed a centralized algorithm based on SCA to solve the WSR maximization problem. Since implementing the centralized is difficult in real networks, we have also developed a distributed algorithm based on Lagrangian dual decomposition and consensus ADMM. Finally, extensive simulation results have been provided to show the effectiveness of the proposed algorithms and that the distributed algorithm can approach the centralized algorithm. Moreover, the results have indicated that the MBCs can enable the operators to realize symbiotic communication in the SAGIN.

## APPENDIX A

### PROOF OF PROPOSITION 1

Let  $F(\mathbf{p}[\tau-1], \mathbf{t}[\tau-1], \mathbf{x}[\tau-1], \tilde{\mathbf{w}}[\tau-1])$  denote the original objective, and  $F_{\mathbf{p}[\tau-1]}(\mathbf{p}[\tau-1], \mathbf{t}[\tau-1], \mathbf{x}[\tau-1], \tilde{\mathbf{w}}[\tau-1])$  denote the approximated objective with the SCA method at point  $\mathbf{p}[\tau-1]$ . For notational simplicity, we use  $F(\mathbf{p}[\tau-1], \tilde{\mathbf{w}}[\tau-1])$  and  $F_{\mathbf{p}[\tau-1]}(\mathbf{p}[\tau-1], \tilde{\mathbf{w}}[\tau-1])$  in the following. In step 4 of Algorithm 1, we have the following inequality

$$\begin{aligned} F(\mathbf{p}[\tau-1], \tilde{\mathbf{w}}[\tau-1]) &\stackrel{(a)}{=} F_{\mathbf{p}[\tau-1]}(\mathbf{p}[\tau-1], \tilde{\mathbf{w}}[\tau-1]) \\ &\stackrel{(b)}{\leq} F_{\mathbf{p}[\tau-1]}(\mathbf{p}[\tau], \tilde{\mathbf{w}}[\tau]) \\ &\stackrel{(c)}{\leq} F(\mathbf{p}[\tau], \tilde{\mathbf{w}}[\tau]) \end{aligned} \quad (43)$$

where (a) comes from the fact that the first-order Taylor expressions used in (14), (17), and (19) are tight at point  $\mathbf{p}[\tau-1]$ ; (b) holds since  $(\mathbf{p}[\tau], \tilde{\mathbf{w}}[\tau])$  are the optimal solutions to (20) with given  $(\mathbf{t}[\tau-1], \mathbf{x}[\tau-1])$ ; and (c) holds since  $F_{\mathbf{p}[\tau-1]}(\mathbf{p}[\tau], \tilde{\mathbf{w}}[\tau])$  is a lower bound of  $F(\mathbf{p}[\tau], \tilde{\mathbf{w}}[\tau])$ .

Note that  $F_{\mathbf{p}[\tau]}(\mathbf{p}[\tau], \tilde{\mathbf{w}}[\tau])$  is the input of step 5, and the inequality (43) can be applied to analyzing step 5 and 6. Finally, we have  $F(\mathbf{p}[\tau-1], \mathbf{t}[\tau-1], \mathbf{x}[\tau-1], \tilde{\mathbf{w}}[\tau-1]) \leq F(\mathbf{p}[\tau], \mathbf{t}[\tau], \mathbf{x}[\tau], \tilde{\mathbf{w}}[\tau])$ , which implies that Algorithm 1 can generate a non-decreasing objective after each iteration. Moreover, the objective is constrained due to the power budget of BSs/STs and the satellite. As a result, Algorithm 1 is guaranteed to converge.

## APPENDIX B

### PROOF OF PROPOSITION 2

In step 3 of Algorithm 6, we have the following inequality

$$F_{\mathbf{p}[\tau-1]}(\mathbf{p}[\tau-1], \tilde{\mathbf{w}}[\tau-1]) \stackrel{(a)}{\leq} F_{\mathbf{p}[\tau-1]}(\mathbf{p}[\tau], \tilde{\mathbf{w}}[\tau]) \quad (44)$$

where (a) comes from the fact that the subproblem (38) is convex with fixed  $(\mathbf{t}, \mathbf{x})$  and consensus ADMM can converge to the optimal solution with enough iterations [43]. Besides, it is clear that (a) also holds when early termination strategy is adopted due to the Algorithm 5 (step 7). The inequality (44) is also applicable for step 4 of Algorithm 6. As a result, we have  $F(\mathbf{p}[\tau-1], \mathbf{t}[\tau-1], \mathbf{x}[\tau-1], \tilde{\mathbf{w}}[\tau-1]) \leq F(\mathbf{p}[\tau], \mathbf{t}[\tau], \mathbf{x}[\tau], \tilde{\mathbf{w}}[\tau])$ .

In step 6 of Algorithm 6, we have the following inequality

$$F_{\mathbf{x}[\tau-1]}(\mathbf{x}[\tau-1]) \stackrel{(b)}{\leq} F_{\mathbf{x}[\tau-1]}(\mathbf{x}[\tau]) \leq F(\mathbf{x}[\tau]) \quad (45)$$

where (b) holds since the subgradient method is guaranteed to converge to the optimal solution when the dual problem (33)

is convex [45]. As a result, we have  $F(\mathbf{p}[\tau-1], \mathbf{t}[\tau-1], \mathbf{x}[\tau-1], \tilde{\mathbf{w}}[\tau-1]) \leq F(\mathbf{p}[\tau], \mathbf{t}[\tau], \mathbf{x}[\tau], \tilde{\mathbf{w}}[\tau])$ , which implies that Algorithm 6 generates a non-decreasing objective after each iteration. Therefore, Algorithm 6 is guaranteed to converge.

## REFERENCES

- [1] ITU, "Framework and overall objectives of the future development of IMT for 2030 and beyond," International Telecommunication Union, Recommendation, 06 2023.
- [2] —, "Measuring digital development: Facts and figures 2022." [Online]. Available: <https://www.itu.int/itu-d/reports/statistics/2022/11/24/ff22-internet-use/>
- [3] J. Liu, Y. Shi, Z. M. Fadlullah, and N. Kato, "Space-air-ground integrated network: A survey," *IEEE Commun. Surveys Tuts.*, vol. 20, no. 4, pp. 2714–2741, May 2018.
- [4] N. Pachler, I. del Portillo, E. F. Crawley, and B. G. Cameron, "An updated comparison of four low earth orbit satellite constellation systems to provide global broadband," in *Proc. IEEE Int. Conf. Commun. (ICC)*, Montreal, Canada, 2021, pp. 1–7.
- [5] B. Di, L. Song, Y. Li, and H. V. Poor, "Ultra-dense LEO: Integration of satellite access networks into 5G and beyond," *IEEE Wireless Commun. Mag.*, vol. 26, no. 2, pp. 62–69, Apr. 2019.
- [6] A. I. Pérez-Neira, M. A. Vázquez, M. B. Shankar, S. Maleki, and S. Chatzinotas, "Signal processing for high-throughput satellites: Challenges in new interference-limited scenarios," *IEEE Signal Process. Mag.*, vol. 36, no. 4, pp. 112–131, Jun. 2019.
- [7] V. Joroughi, M. A. Vázquez, and A. I. Pérez-Neira, "Generalized multicast multibeam precoding for satellite communications," *IEEE Trans. Wireless Commun.*, vol. 16, no. 2, pp. 952–966, Dec. 2016.
- [8] W. Wang, L. Gao, R. Ding, J. Lei, L. You, C. A. Chan, and X. Gao, "Resource efficiency optimization for robust beamforming in multi-beam satellite communications," *IEEE Trans. Veh. Technol.*, vol. 70, no. 7, pp. 6958–6968, Jun. 2021.
- [9] A. Abdi, W. C. Lau, M.-S. Alouini, and M. Kaveh, "A new simple model for land mobile satellite channels: First-and second-order statistics," *IEEE Trans. Wireless Commun.*, vol. 2, no. 3, pp. 519–528, May 2003.
- [10] D.-H. Na, K.-H. Park, Y.-C. Ko, and M.-S. Alouini, "Performance analysis of satellite communication systems with randomly located ground users," *IEEE Trans. Wireless Commun.*, vol. 21, no. 1, pp. 621–634, Jul. 2021.
- [11] E. Kim, I. P. Roberts, and J. G. Andrews, "Downlink analysis and evaluation of multi-beam LEO satellite communication in shadowed rician channels," *IEEE Trans. Veh. Technol.*, Sep. 2023.
- [12] P. Gu, R. Li, C. Hua, and R. Tafazolli, "Dynamic cooperative spectrum sharing in a multi-beam LEO-GEO co-existing satellite system," *IEEE Trans. Wireless Commun.*, vol. 21, no. 2, pp. 1170–1182, Aug. 2021.
- [13] X. Hu, S. Liu, R. Chen, W. Wang, and C. Wang, "A deep reinforcement learning-based framework for dynamic resource allocation in multibeam satellite systems," *IEEE Commun. Lett.*, vol. 22, no. 8, pp. 1612–1615, Jun. 2018.
- [14] A. Wang, L. Lei, E. Lagunas, A. I. Pérez-Neira, S. Chatzinotas, and B. Ottersten, "NOMA-enabled multi-beam satellite systems: Joint optimization to overcome offered-requested data mismatches," *IEEE Trans. Veh. Technol.*, vol. 70, no. 1, pp. 900–913, Dec. 2020.
- [15] C. Li, H. Zhu, J. Tang, J. Hu, and G. Li, "User grouping in multiuser satellite MIMO downlink with fairness consideration," *IEEE Wireless Commun. Lett.*, vol. 11, no. 8, pp. 1575–1579, Apr. 2022.
- [16] T-Mobile, "T-Mobile Takes Coverage Above and Beyond With SpaceX." [Online]. Available: <https://www.t-mobile.com/news/un-carrier/t-mobile-takes-coverage-above-and-beyond-with-spacex>
- [17] Q. Wang, H. Zhang, J.-B. Wang, F. Yang, and G. Y. Li, "Joint beamforming for integrated mmwave satellite-terrestrial self-backhauled networks," *IEEE Trans. Veh. Technol.*, vol. 70, no. 9, pp. 9103–9117, Jul. 2021.
- [18] Y.-C. Liang, J. Tan, H. Jia, J. Zhang, and L. Zhao, "Realizing intelligent spectrum management for integrated satellite and terrestrial networks," *J. Commun. and Inf. Netw.*, vol. 6, no. 1, pp. 32–43, Mar. 2021.
- [19] F. Lyu, P. Yang, H. Wu, C. Zhou, J. Ren, Y. Zhang, and X. Shen, "Service-oriented dynamic resource slicing and optimization for space-air-ground integrated vehicular networks," *IEEE Trans. Intell. Transp. Syst.*, vol. 23, no. 7, pp. 7469–7483, Apr. 2021.
- [20] Y. Zhang, H. Zhang, H. Zhou, K. Long, and G. K. Karagiannidis, "Resource allocation in terrestrial-satellite-based next generation multiple access networks with interference cooperation," *IEEE J. Sel. Areas Commun.*, vol. 40, no. 4, pp. 1210–1221, Jan. 2022.
- [21] X. Li, W. Feng, Y. Chen, C.-X. Wang, and N. Ge, "Maritime coverage enhancement using uavs coordinated with hybrid satellite-terrestrial networks," *IEEE Trans. Commun.*, vol. 68, no. 4, pp. 2355–2369, Jan. 2020.
- [22] A. Alsharoa and M.-S. Alouini, "Improvement of the global connectivity using integrated satellite-airborne-terrestrial networks with resource optimization," *IEEE Trans. Wireless Commun.*, vol. 19, no. 8, pp. 5088–5100, Apr. 2020.
- [23] S. Liu, H. Dahrouj, and M.-S. Alouini, "Joint user association and beamforming in integrated satellite-haps-ground networks," *IEEE Trans. Veh. Technol.*, Nov. 2023.
- [24] B. Di, H. Zhang, L. Song, Y. Li, and G. Y. Li, "Ultra-dense LEO: Integrating terrestrial-satellite networks into 5G and beyond for data offloading," *IEEE Trans. Wireless Commun.*, vol. 18, no. 1, pp. 47–62, Dec. 2018.
- [25] D. Han, Q. Ye, H. Peng, W. Wu, H. Wu, W. Liao, and X. Shen, "Two-timescale learning-based task offloading for remote IoT in integrated satellite-terrestrial networks," *IEEE Internet Things J.*, vol. 10, no. 12, pp. 10 131–10 145, Jan. 2023.
- [26] R. Deng, B. Di, S. Chen, S. Sun, and L. Song, "Ultra-dense LEO satellite offloading for terrestrial networks: How much to pay the satellite operator?" *IEEE Trans. Wireless Commun.*, vol. 19, no. 10, pp. 6240–6254, Jun. 2020.
- [27] Y.-C. Liang, R. Long, Q. Zhang, and D. Niyato, "Symbiotic communications: Where Marconi meets Darwin," *IEEE Wireless Commun. Mag.*, vol. 29, no. 1, pp. 144–150, Feb. 2022.
- [28] R. Long, Y.-C. Liang, H. Guo, G. Yang, and R. Zhang, "Symbiotic radio: A new communication paradigm for passive internet of things," *IEEE Internet of Things Journal*, vol. 7, no. 2, pp. 1350–1363, Nov. 2020.
- [29] H. Zhou, Q. Zhang, Y.-C. Liang, and Y. Pei, "Assistance-transmission tradeoff for RIS-assisted symbiotic radios," *IEEE Trans. Wireless Commun.*, Nov. 2023.
- [30] Q. Zhang, H. Zhou, Y.-C. Liang, W. Zhang, and H. V. Poor, "Channel capacity of RIS-assisted symbiotic radios with imperfect knowledge of channels," *IEEE Trans. on Cogn. Commun. Netw.*, Mar. 2024.
- [31] J. Wang, Y.-C. Liang, and S. Sun, "Multi-user multi-IoT-device symbiotic radio: A novel massive access scheme for cellular IoT," *IEEE Trans. Wireless Commun.*, Apr. 2024.
- [32] H. Chen, R. Long, and Y.-C. Liang, "Transmission protocol and beamforming design for RIS-assisted symbiotic radio over OFDM carriers," in *Proc. IEEE Global Commun. Conf. (GLOBECOM)*, Kuala Lumpur, Malaysia, 2023, pp. 3258–3263.
- [33] J. Tan, S. Xiao, S. Han, Y.-C. Liang, and V. C. M. Leung, "QoS-aware user association and resource allocation in LAA-LTE/WiFi coexistence systems," *IEEE Trans. Wireless Commun.*, vol. 18, no. 4, pp. 2415–2430, Mar. 2019.
- [34] S. He, J. Ge, and Y.-C. Liang, "User association for symbiotic spectrum and service sharing among multiple mobile network operators," *IEEE Trans. Wireless Commun.*, Jul. 2023.
- [35] —, "Joint user association and beamforming design in multi-operator networks: A symbiotic communication perspective," in *Proc. IEEE Global Commun. Conf. (GLOBECOM)*, Kuala Lumpur, Malaysia, 2023, pp. 1–6.
- [36] R. Cheng, Y. Sun, L. Mohjazi, Y.-C. Liang, and M. Imran, "Blockchain-assisted intelligent symbiotic radio in space-air-ground integrated networks," *IEEE Netw.*, vol. 37, no. 2, pp. 94–101, Sep. 2023.
- [37] M. Razaviyayn, M. Hong, and Z.-Q. Luo, "A unified convergence analysis of block successive minimization methods for nonsmooth optimization," *SIAM J. Optim.*, vol. 23, no. 2, pp. 1126–1153, 2013.
- [38] B. Khamidehi, A. Rahmati, and M. Sabbaghian, "Joint sub-channel assignment and power allocation in heterogeneous networks: An efficient and distributed method," *IEEE Commun. Lett.*, vol. 20, no. 12, pp. 2490–2493, Aug. 2016.
- [39] M. Sanjabi, M. Razaviyayn, and Z.-Q. Luo, "Optimal joint base station assignment and beamforming for heterogeneous networks," *IEEE Trans. Signal Process.*, vol. 62, no. 8, pp. 1950–1961, Jan. 2014.
- [40] O. Tervo, L.-N. Tran, H. Pannanen, S. Chatzinotas, B. Ottersten, and M. Juntti, "Energy-efficient multicell multigroup multicasting with joint beamforming and antenna selection," *IEEE Trans. Signal Process.*, vol. 66, no. 18, pp. 4904–4919, Aug. 2018.
- [41] Q. Ye, B. Rong, Y. Chen, M. Al-Shalash, C. Caramanis, and J. G. Andrews, "User association for load balancing in heterogeneous cellular networks," *IEEE Trans. Wireless Commun.*, vol. 12, no. 6, pp. 2706–2716, Apr. 2013.
- [42] K. Shen and W. Yu, "Distributed pricing-based user association for downlink heterogeneous cellular networks," *IEEE J. Sel. Areas Commun.*, vol. 32, no. 6, pp. 1100–1113, Jun. 2014.

- [43] S. Boyd, N. Parikh, E. Chu, B. Peleato, J. Eckstein *et al.*, “Distributed optimization and statistical learning via the alternating direction method of multipliers,” *Foundations and Trends® in Machine learning*, vol. 3, no. 1, pp. 1–122, 2011.
- [44] K.-G. Nguyen, L.-N. Tran, Q.-D. Vu, and M. Juntti, “Distributed energy efficiency fairness optimization by ADMM in multicell MISO downlink,” in *Proc. IEEE Int. Conf. Commun. (ICC)*, Kuala Lumpur, Malaysia, 2016, pp. 1–6.
- [45] S. Boyd, L. Xiao, and A. Mutapcic, “Subgradient methods,” *lecture notes of EE392o, Stanford University, Autumn Quarter*, vol. 2004, no. 01, 2003.